Dynamic Light Scattering of a Flexible Highly Charged Polyelectrolyte in the Dilute Concentration Regime

J. J. Tanahatoe and M. E. Kuil*

Leiden Institute of Chemistry, Gorlaeus Laboratories, Section Physical and Macromolecular Chemistry, Leiden University, P.O. Box 9502, 2300 RA Leiden, The Netherlands

Received March 11, 1997; Revised Manuscript Received May 20, 1997[⊗]

ABSTRACT: The diffusion behavior of the flexible highly charged polyelectrolyte sodium poly(styrenesulfonate) has been studied extensively with dynamic light scattering in the dilute concentration regime. The apparent diffusion coefficient was determined for one molar mass and five ionic strengths at dilute polyelectrolyte concentrations. The apparent diffusion coefficients extrapolated to zero polyelectrolyte concentration were compared with theoretical D_0 values calculated with a theoretical procedure based on a wormlike chain model, including the persistence length, the excluded volume, and counterion condensation. A satisfactory agreement was found. From the polyelectrolyte concentration dependence of the apparent diffusion coefficient, the diffusion second virial coefficient could be obtained. The ionic strength dependence of the diffusion second virial coefficient k_d was found to be linearly proportional to $1/c_s$, in agreement with the prediction of small ion−polyion coupled mode theories.

Introduction

In polymer and polyelectrolyte solutions at least two concentration regimes can be distinguished: the dilute and the semidilute regime. The transition between these two regimes is not sharp but shows a transition regime around the critical overlap concentration. These different concentration regimes and the critical concentration have been theoretically described by de Gennes[1] and Odijk.[2] In the dilute concentration regime individual chains can be distinguished, whereas in the semidilute regime the chains interpenetrate.

The Brownian motion of the macromolecular chain can be experimentally studied by dynamic light scattering. From the autocorrelation function of the scattered light, one can obtain the dynamic structure factor.[3] This dynamic structure factor gives the apparent diffusion coefficient of the average individual chain.

A strong polyelectrolyte in solution dissociates fully into a polyion and numerous counterions. The addition of low molar mass electrolyte results in the screening of the electric charges on the polyion. The conformation of the polyion depends on the screening of the charges. The persistence length of a polyelectrolyte characterizes the effective rigidity of the polyelectrolyte chain and involves short range electrostatic interactions. Long range electrostatic interactions are involved in the excluded volume.

The apparent diffusion coefficient of a polyelectrolyte in the dilute concentration regime depends on the chain length, ionic strength, linear charge density, polyelectrolyte concentration, and chemical structure. Several researchers[4−8] have reported apparent diffusion coefficients of flexible highly charged polyelectrolytes in the dilute concentration regime. In this work apparent diffusion coefficients of the strong polyelectrolyte sodium poly(styrenesulfonate) were obtained in aqueous solutions for one molar mass at five different ionic strengths in the dilute regime. From the polyelectrolyte concentration dependence of the apparent diffusion coefficient, values for D_0, the apparent diffusion coefficient extrapolated to zero polyelectrolyte concentration, and k_d, the diffusion second virial coefficient, were obtained. The experimental D_0 values were compared with theoretical values, calculated with a theoretical procedure based on a wormlike chain model, including the persistence length, the excluded volume, and counterion condensation. The experimentally ionic strength dependence of the diffusion second virial coefficient was qualitatively confronted with small ion−polyion coupled mode theories.

Experimental Section

Sodium poly(styrenesulfonate) with a molar mass of 77.4 kg/mol was purchased from Viscotek Benelux. The M_w/M_n ratio of the polyelectrolyte was smaller than 1.2. Nondialyzed samples contain a certain amount of sodium sulfate, and purification is necessary. In the purification procedure 1 g of NaPSS is dissolved in 0.2 M HCl (Baker Chemical Co.). This solution is dialyzed in a Visking seamless cellulose tubing against water, which was purified by a Milli-Q system. The dialysis bag was purified by heating in a solution of sodium bicarbonate (Merck), EDTA (Merck), and Millipore water, followed by extensive rinsing with Millipore water. The water surrounding the dialysis tube is refreshed several times, until the electric conductivity of this water equals the conductivity of pure water (the conductivity was always smaller than 1 μS/cm). Subsequently, the dialyzed solution is converted to the sodium salt of PSS by potentiometric titration with 0.1 M NaOH (Titrisol) and the solution is stored freeze dried. Ultrapure salt solutions were prepared by dissolving NaCl (Merck) in Millipore water. NaPSS solutions were prepared by dissolving the freeze-dried NaPSS in a salt solution. All samples were filtered through a Millipore GV 0.22 μm pore size filter, prior to the light scattering experiment. After the light scattering experiment, the concentrations of the samples were determined spectrophotometrically at a wavelength of 261.5 nm, using an extinction coefficient of 1.92 ± 0.03 L g^{-1} cm^{-1}. The extinction coefficient was determined using the freeze-dried NaPSS. Infrared absorbance measurements were employed to determine the water content of the freeze-dried NaPSS, and the extinction coefficient was corrected accordingly.

Dynamic Light Scattering. Dynamic light scattering measurements on the NaPSS solutions were performed using an ALV goniometer (ALV, Langen, Germany) in combination with an ALV-5000 fast correlator and a photomultiplier. The light source was an argon-ion laser (Spectra Physics model 2020-03), operating at a wavelength of 514.5 nm in the light stabilized mode. The filtered NaPSS solutions go directly into a cylindrical quartz cuvette with an outer diameter of 2 cm. Before and during each measurement the solution was ther-

[⊗] Abstract published in *Advance ACS Abstracts,* September 1, 1997.

S0024-9297(97)00325-2 CCC: $14.00

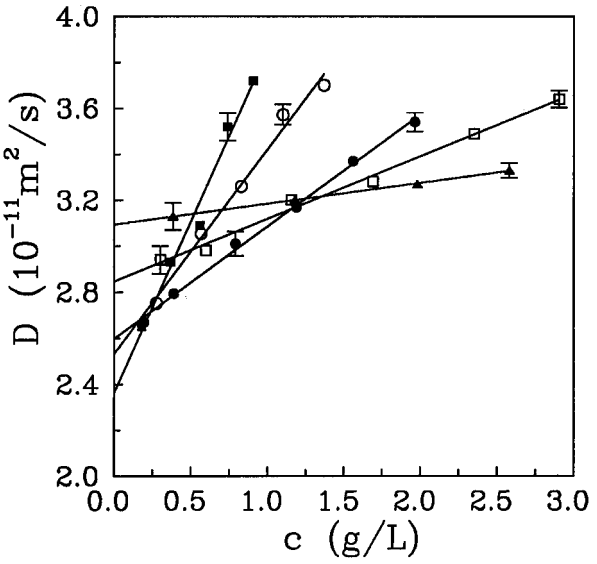

Figure 1. Apparent diffusion coefficient as a function of the NaPSS concentration for five ionic strengths: (■) c_s = 0.01 M; (○) c_s = 0.02 M; (●) c_s = 0.05 M; (□) c_s = 0.1 M; (▲) c_s = 0.5 M. The molar mass is 77.4 kg/mol. Drawn lines are linear least squares best fits.

mostated at a temperature of 25 °C. Before each experiment the filtration setup and the quartz cuvette were cleaned with 0.1 M NaOH and extensively flushed with Millipore water. To check if the filtration setup and the cuvette were clean, Millipore water was filtered in a cuvette. After thermostating this water, the intensity autocorrelation function was measured. If this autocorrelation function does not show any decay time in the multiple τ mode, the filtration setup and the cuvette are considered clean and the NaPSS solution was filtered.

Analysis of the Dynamic Light Scattering Data. The ALV 5000 correlator calculates the normalized intensity autocorrelation function $g^{(2)}(\tau)$. The intensity autocorrelation functions measured in this investigation all deviate moderately from the exponential form. For all measurements we have used a third order cumulant expansion:[7]

$$g^{(2)}(\tau) = 1 + B \exp\left(-2\langle\Gamma\rangle\tau + \frac{2\mu_2}{2!\langle\Gamma\rangle^2}(\langle\Gamma\rangle\tau)^2 - \frac{2\mu_3}{3!\langle\Gamma\rangle^3}(\langle\Gamma\rangle\tau)^3\right) \quad (1)$$

$\langle\Gamma\rangle$ is the average decay rate, μ_n is the nth order moment of the distribution of decay rates, and B is an equipment dependent amplitude factor. For a relatively narrow distribution of decay rates, the apparent diffusion coefficient is given by

$$D = \frac{\langle\Gamma\rangle}{q^2} \quad (2)$$

q is the magnitude of the scattering vector, defined as $q = (4\pi n_s/\lambda_0)\sin(\theta/2)$ with n_s the refractive index of the solvent, λ_0 the wavelength of the incident light in vacuo and θ the scattering angle. A fit is considered satisfactory if there are no systematic deviations in the plot of the residuals of the fitted curve. All samples were measured over the angular range from 30° up to 150° with 10° increments. From the linear least squares fit of $\langle\Gamma\rangle$ versus q^2 the apparent diffusion coefficients were obtained.

Results and Discussion

Figure 1 shows the apparent diffusion coefficient of one molar mass (M = 77.4 kg/mol) as a function of the polyelectrolyte concentration for five different ionic strengths. In sufficiently dilute polyelectrolyte solutions it is observed that the apparent diffusion coefficient measured with dynamic light scattering is a linear function of the polyelectrolyte concentration:

$$D = D_0(1 + k_d c) \quad (3)$$

with D the apparent diffusion coefficient, D_0 the apparent diffusion coefficient at infinite dilution, k_d the diffusion second virial coefficient, and c the polyelectrolyte concentration. The separation between the dilute virial regime and the semidilute regime is indicated by the critical overlap concentration.[1,2] In this work the experiments were performed well below the molar mass and ionic strength dependent, critical overlap concentration.

Table 1. Apparent Diffusion Coefficient at Infinite Dilution, the Diffusion Second Virial Coefficient, the Total Persistence Length According to Le Bret, and Theoretical D_0 Values without and with Excluded Volume for Five Ionic Strengths

c_s (M)	D_0^{exp} (10^{-11} m^2/s)	k_d (mL/g)	L_t (Å)[a]	D_0 (10^{-11} m^2/s)[b]	D_0 (10^{-11} m^2/s)[c]
0.01	2.36 ± 0.07	636 ± 55	66.0	3.05	2.33
0.02	2.52 ± 0.05	354 ± 22	48.5	3.31	2.52
0.05	2.59 ± 0.01	188 ± 5	33.7	3.70	2.83
0.1	2.85 ± 0.02	96 ± 5	26.6	3.99	3.09
0.5	3.09 ± 0.003	29 ± 1	17.9	4.48	3.40

[a] Calculated with L_0=12 Å. [b] Calculated without excluded volume. [c] Calculated with excluded volume.

For each ionic strength we have determined the apparent diffusion coefficient for several polyelectrolyte concentrations in the dilute regime. The polyelectrolyte concentration dependence of the apparent diffusion coefficient is linear for all conditions employed and shows that the virial expansion can be limited to the diffusion second virial coefficient in the concentration range studied. Figure 1 shows that on decreasing the ionic strength the polyelectrolyte concentration dependence of the apparent diffusion coefficient becomes stronger.

The drawn lines in Figure 1 are linear least squares best fits, and values for D_0, the apparent diffusion coefficient extrapolated to zero polyelectrolyte concentration, could be obtained. The slope of each line divided by D_0 gives us according to eq 3 the diffusion second virial coefficient k_d. The obtained values for D_0 and k_d are collected in Table 1.

The ionic strength dependence of the apparent diffusion coefficient extrapolated to zero polyelectrolyte concentration for NaPSS with M = 77.4 kg/mol is depicted in Figure 2. With decreasing ionic strength, D_0 becomes smaller due to expansion of the polyelectrolyte coil. To give a detailed interpretation of our experimental D_0 values, we will give a procedure to calculate theoretical D_0 values. The theoretical diffusion coefficient at infinite dilution D_0 is related to the friction coefficient f by the Einstein relation

$$D_0 = \frac{k_b T}{f} \quad (4)$$

where k_b is the Boltzmann constant and T is the absolute temperature. The friction coefficient f of an excluded volume chain can be written as

$$f = \alpha_h f_0 \quad (5)$$

with f_0 the friction coefficient without excluded volume and α_h the hydrodynamic expansion factor. Yamakawa and Fujii[9] have derived a procedure to calculate the

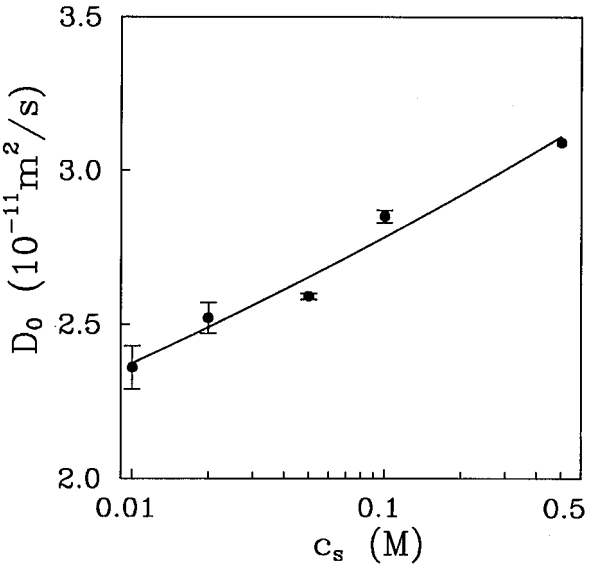

Figure 2. Apparent diffusion coefficient at infinite dilution D_0 as a function of the ionic strength. The molar mass is 77.4 kg/mol. The drawn line is the linear least squares best fit.

translational friction coefficient of a wormlike chain of finite thickness without excluded volume by applying the Oseen−Burgers procedure of hydrodynamics to wormlike cylinder models. The wormlike chain is represented as a flexible cylinder with contour length L and radius r. Their expression for the translational friction coefficient f_0 for the wormlike chain with N_k Kuhn lengths reads for $N_k > 2.278$

$$\frac{3\pi\eta_0 L}{f_0} = A_1 N_k^{1/2} + A_2 + A_3 N_k^{-1/2} + A_4 N_k^{-1} + A_5 N_k^{-3/2} \quad (6)$$

and for $N_k \leq 2.278$

$$\frac{3\pi\eta_0 L}{f_0} = C_1 \ln\left(\frac{N_k}{d}\right) + C_2 + C_3 N_k + C_4 N_k^2 + C_5 N_k^3 + C_6\left(\frac{d}{N_k}\right)\ln\left(\frac{N_k}{d}\right) + C_7\left(\frac{d}{N_k}\right) + C_8\left(\frac{d}{N_k}\right)^2 + C_9\left(\frac{d}{N_k}\right)^3 + C_{10}\left(\frac{d}{N_k}\right)^4 \quad (7)$$

with η_0 the viscosity of the solvent. The coefficients $A_1...A_5$ and $C_1...C_{10}$, which are functions of the reduced diameter $d = r/L_t$, are given in ref 9. The number of Kuhn lengths $N_k = L/2L_t$ with L_t the total persistence length.

In eq 5 α_h is the hydrodynamic expansion factor, which depends on the excluded volume parameter z

$$z = \frac{3^{3/2}}{32\pi^{3/2}}\beta L^{1/2} L_t^{-7/2} \quad (8)$$

The excluded volume β between Kuhn segments with length $2L_t$ is approximated as $\beta = \beta_0 + \beta_e$, where β_0 represents hard-core interactions and β_e electrostatic interactions. The hard-core part[10] is given by $\beta_0 = 4\pi L_t^2 r$ with r the radius of a rod segment. Fixman and Skolnick[11] have calculated for the binary cluster integral β_e

$$\beta_e \simeq 8 L_t^2 \kappa^{-1} R(\omega) \quad (9)$$

where $R(\omega)$ is given as

$$R(\omega) = \int_0^{\pi/2} \sin^2\theta \int_0^{\omega/\sin\theta} x^{-1}(1 - e^{-x})\, dx\, d\theta \quad (10)$$

with $\omega = (2\pi/Q)\kappa^{-1}e^{-2\kappa r}$, assuming Manning's counterion condensation.[12] In eq 9 κ^{-1} is the Debye−Hückel screening length. The Bjerrum length $Q = 7.135$ Å for water at 25 °C. To calculate the expansion factor α_h, we can use the Barrett equation[13]

$$\alpha_h = (1 + 6.09z + 3.59z^2)^{0.1} \quad (11)$$

To calculate theoretical D_0 values, values for the total persistence lengths and a value for the radius r of the polyion are needed. We use a value of 9 Å for the radius of NaPSS. This value can be estimated from the bond lengths in NaPSS by taking into account a possible layer of water molecules or counterions around the polyelectrolyte chain. For polyelectrolytes the total persistence length L_t is written as[14]

$$L_t = L_0 + L_e \quad (12)$$

The total persistence length represents the effective rigidity of the polyelectrolyte as the sum of two contributions: the intrinsic persistence length L_0 due to the rigidity of the uncharged chain and the electrostatic persistence length L_e arising from the repulsion between the ionic sites.

Odijk[14] and Skolnick and Fixman[15] (OSF) derived independently an expression for the electrostatic persistence length for a line charge on the basis of a linearized form of the Poisson−Boltzmann equation

$$L_e = \frac{1}{12} Q\left(\frac{Na}{Q}\right)^2 (e^{-y}(y^{-1} + 5y^{-2} + 8y^{-3}) + 3y^{-2} - 8y^{-3}) \quad (13)$$

$y = \kappa L$, and N is the number of elementary charges along the chain. The contour length of the polyelectrolyte $L = a \times M/M_m$, with a the monomer contour length and M_m the monomer mass, which is 206.19 g/mol for NaPSS.

Le Bret[16] has calculated the electrostatic persistence length for a toroid by a numerical procedure on the basis of the complete Poisson−Boltzmann equation. His results for the electrostatic persistence length are given in Tables I and II of ref 16 as a function of the polyion radius, the Debye−Hückel screening length, and the charge parameter. The data in his Tables I and II are calculated for a polyion radius of 10 Å. The electrostatic persistence length can be calculated for other values of the polyion radius. For Manning's counterion condensation the charge parameter is 1 and we have calculated the electrostatic persistence lengths for a polyion radius of 9 Å in the ionic strength range that spans our ionic strength range. From interpolation of these data the electrostatic persistence lengths at our ionic strengths were obtained.

Now we are able to calculate theoretical D_0 values. For the intrinsic persistence length a value of 12 Å[17,18] is used. We cannot apply the OSF persistence length calculation since the OSF electrostatic persistence length is not a perturbation of the intrinsic persistence length for most ionic strengths employed. Moreover, the OSF electrostatic persistence length has been derived for a line charge while our theoretical procedure views the polyelectrolyte as a wormlike chain of finite thickness. Therefore, we apply the electrostatic persistence

length calculation of Le Bret. Theoretically calculated D_0 values using the persistence lengths according to Le Bret, with and without the excluded volume correction, are summarized in Table 1. The monomer contour distance was 2.5 Å. The radius of the polyion is set to 9 Å, taking into account a possible layer of water molecules or counterions around the polyelectrolyte chain. A change in the D_0 value of about 3% is found when this radius varied between 8 and 10 Å. The calculated D_0 values without excluded volume correction are much larger than the experimental D_0 values. Correction for the excluded volume effect leads to values that are close to the experimental values. Especially at our lowest ionic strengths the agreement is remarkable. At our high ionic strengths the theoretical values are about 10% larger than the experimental ones.

The polyelectrolyte is viewed as a chain consisting of rodlike segments with radius r and length $2L_t$. It could be conceived that the amount of condensed counterions depends on the length of the rodlike chain segment, since the application of the Manning counterion condensation theory is strictly speaking only valid for infinitely long rods. Increasing the ionic strength, the total persistence length decreases and the chain segment length decreases while the number of chain segments increases. In this case the amount of condensed counterions will be smaller due to a decreasing segment length and the effective linear charge density increases. We note that a value larger than $1/Q$ for the effective linear charge density at our highest ionic strength yields a smaller value for D_0 and the deviation from the experimental value becomes smaller. This is an indication that the Manning counterion condensation model breaks down for flexible chains.

The excluded volume β in eq 8 is valid for $L_t \gg r$. This means that the rodlike segments must be rodlike. From the total persistence lengths in Table 1 it is seen that the validity of this condition becomes more questionable as the ionic strength increases. For example, at our highest ionic strength the total persistence length is about 18 Å, so the chain segment has a length of 36 Å and a diameter of 18 Å.

We have given two possible explanations for the remaining discrepancies we found between the theoretical and experimental D_0 values at high ionic strengths. First, at high ionic strengths the counterion condensation model according to Manning is not correct, and secondly, the excluded volume correction becomes questionable. These two phenomena occur simultaneously due to decreasing segment length and increasing number of segments as the ionic strength increases.

In our theoretical procedure to calculate D_0 we have used a value of 2.5 Å for the monomer contour length. Van der Maarel et al.[19] and Kassapidou et al.[20] have determined with small angle neutron scattering on semidilute PSS solutions without added salt a value of about 1.7 Å for the z-axis projected distance between monomers. We have also used this value for the monomer contour length in all our theoretical calculations. The theoretical D_0 values with the excluded volume correction then lead to values that are much larger than the experimental D_0 values. Recently, Spiteri et al.[21] have determined with small angle neutron scattering on semidilute PSS solutions with added salt a monomer contour length of 2.46 Å, very close to the value of 2.5 Å.

Figure 3 shows that the experimental diffusion second virial coefficient is a linear function of $1/c_s$. The dependence of k_d on $1/c_s$ is predicted by the small ion−polyion coupled mode theory, as reviewed by Schurr and Schmitz.[22] The molecular theory of Imai and Mandel[23,24] also predicts this. Since this is not obvious at first sight, we will elaborate this in some detail below. Imai and Mandel have derived a molecular theory for the effective diffusion coefficient of polyelectrolytes with excess added salt. The theory is only valid in dilute solutions. The approximate expression[24] obtained for the effective diffusion coefficient up to the linear terms in the polyelectrolyte concentration is

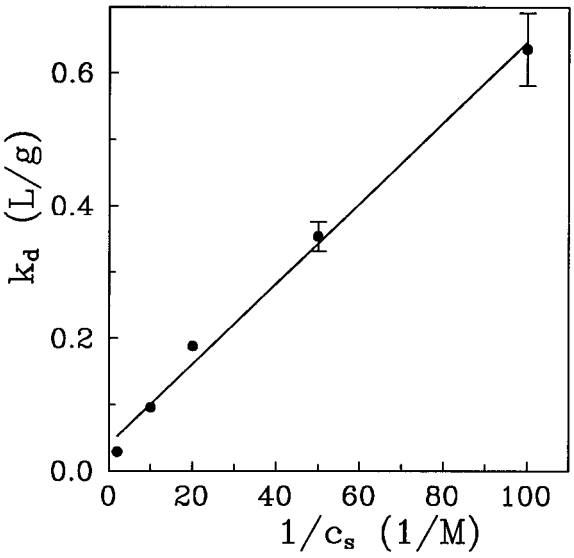

Figure 3. Diffusion second virial coefficient k_d as a function of the reciprocal ionic strength. The molar mass is 77.4 kg/mol. The drawn line is the linear least squares best fit.

$$\frac{D}{k_b T} \simeq \frac{\frac{M}{N_a}\frac{\partial \Pi/k_b T}{\partial c}}{(\omega_p + \omega_s)}\left(1 + \frac{{\gamma_p}^2 Z^2}{M}\left[1 - \frac{\omega_\pm}{\omega_p + \omega_s}\right]\frac{c}{2c_s} + ...\right) \tag{14}$$

with Π the osmotic pressure of the polyelectrolyte solution, M the molar mass of the polyelectrolyte, Z the number of elementary charges on the polyion, c_s the added salt concentration, γ_p the activity coefficient of the counterions in the salt-free solution, k_b the Boltzmann constant, T the absolute temperature, N_a Avogadro's number, and ω_p the friction coefficient of the polyelectrolyte. The friction coefficients of the small coions and counterions, $\omega_\pm$, are assumed to have identical values. The definition of ω_s is more complicated, but it is proportional to, and of the same order as, $\omega_\pm$.

Equation 14 contains the derivative of Π with respect to c. The classic virial expansion for the osmotic pressure is

$$\frac{M\Pi}{N_a k_b T} = c(1 + A_2 M c + ...) \tag{15}$$

with A_2 the osmotic second virial coefficient. For very dilute solutions the osmotic second virial coefficient contribution can be neglected (i.e., the osmotic pressure is well represented by the van't Hoff expression). Substituting reasonable estimates for the parameters in the term A_2Mc, we can estimate this contribution. A typical value[8,25] for the osmotic second virial coefficient of NaPSS in 0.01 M NaCl is of the order of 10^{-3} mol mL g^{-2}. The estimated value for the term A_2Mc is about

0.04. Higher ionic strengths than 0.01 M lead to estimated values for the term A_2Mc that are smaller than 0.04. If the term A_2Mc is neglected, $(M/N_a)\partial(\Pi/k_BT)/\partial c$ in eq 14 equals unity, so the theoretical diffusion second virial coefficient as defined by eq 3 is well approximated by

$$k_d \simeq \frac{\gamma_p^2 Z^2}{2Mc_s}\left[1 - \frac{\omega_\pm}{\omega_p + \omega_s}\right] \qquad (16)$$

It is likely that the polyion friction coefficient ω_p is much larger than ω_s or $\omega_\pm$, so the value between square brackets will only slightly deviate from 1. The activity coefficient γ_p of the counterions in a salt-free solution does not depend on the ionic strength, according to its definition. Equation 16 shows that k_d is proportional to $1/c_s$. The $1/c_s$ dependence of k_d was also experimentally found by Smits et al.[7] for the linear highly charged polyelectrolyte poly(ethylenimine).

Conclusions

The polyelectrolyte concentration dependence of the apparent diffusion coefficient of NaPSS is linear in the dilute concentration regime and is strongly dependent on the ionic strength.

The experimentally determined apparent diffusion coefficients at infinite dilution were compared with theoretical values calculated with a theoretical procedure based on a wormlike chain model, including the persistence length, the excluded volume, and counterion condensation. For all ionic strengths a satisfactory agreement was found.

The experimental ionic strength dependence of the diffusion second virial coefficient is in agreement with the prediction of small ion−polyion coupled mode theories and earlier experiments on highly charged polyelectrolytes.

Acknowledgment. We gratefully acknowledge Prof. T. Odijk and Dr. J. R. C van der Maarel for stimulating discussions. This research was supported by the Netherlands Foundation for Chemical Research (SON) with financial aid from the Netherlands Organization for the Advancement of Research (NWO).

References and Notes

(1) de Gennes, P. G. *Scaling concepts in polymer physics*; Cornell University Press: Ithaca, New York, 1979.
(2) Odijk, T. *Macromolecules* **1979**, *12*, 688.
(3) Doi, M.; Edwards, S. F. *The Theory of Polymer Dynamics*; Oxford University Press: Oxford, U.K., 1986.
(4) Koene, R. S.; Nicolai, T.; Mandel, M. *Macromolecules* **1983**, *16*, 227.
(5) Wang, L.; Yu, H. *Macromolecules* **1988**, *21*, 3498.
(6) Peitzsch, R. M.; Burt, M. J.; Reed, W. F. *Macromolecules* **1992**, *25*, 806.
(7) Smits, R. G.; Kuil, M. E.; Mandel, M. *Macromolecules* **1993**, *26*, 6808.
(8) Borochov, N.; Eisenberg, H. *Macromolecules* **1994**, *27*, 1440.
(9) Yamakawa, H.; Fujii, M. *Macromolecules* **1973**, *6*, 407.
(10) Tanford, C. *Physical Chemistry of Macromolecules*; John Wiley and Sons: New York, 1961.
(11) Fixman, M.; Skolnick, J. *Macromolecules* **1978**, *11*, 863.
(12) Manning, G. S. *J. Chem. Phys.* **1969**, *51*, 924.
(13) Barrett, A. J. *Macromolecules* **1984**, *17*, 1561.
(14) Odijk, T. *J. Polym. Sci., Polym. Phys. Ed.* **1977**, *15*, 477
(15) Skolnick, J.; Fixman, M. *Macromolecules* **1977**, *10*, 944.
(16) Le Bret, M. *J. Chem. Phys.* **1982**, *76*, 6243.
(17) Nierlich, M.; Boué, F.; Lapp, A.; Oberthür, R. *Colloid Polym. Sci.* **1985**, *263*, 955.
(18) Weill, G.; Maret, G. *Polymer* **1982**, *23*, 1990.
(19) van der Maarel, J. R. C.; Groot, L. C. A.; Hollander, J. G.; Jesse, W.; Kuil, M.E.; Leyte, J. C.; Leyte-Zuiderweg, L. H.; Mandel, M.; Cotton, J. P.; Jannink, G.; Lapp, A.; Farago, B. *Macromolecules* **1993**, *26*, 7295.
(20) Kassapidou, K.; Jesse, W.; Kuil, M. E.; Lapp, A; Egelhaaf, S.; van der Maarel, J. R. C. *Macromolecules* **1997**, *30*, 2671.
(21) Spiteri, M. N.; Boué, F.; Lapp, A.; Cotton, J. P. *Phys. Rev. Lett.* **1996**, *77*, 5218.
(22) Schurr, J. M.; Schmitz, K. S. *Annu. Rev. Phys. Chem.* **1986**, *37*, 271.
(23) Imai, N.; Mandel, M. *Macromolecules* **1982**, *15*, 1562.
(24) Mandel, M. *Physica* **1987**, *147A*, 99.
(25) Takahashi, A.; Kato, T.; Nagasawa, M. *J. Phys. Chem.* **1967**, *71*, 2001.

MA9703259